Photonic band gaps in a two-dimensional hybrid triangular-graphite lattice

L. J. Martínez, A. García-Martín and P. A. Postigo

Instituto de Microelectrónica de Madrid, Centro Nacional de Microelectrónica, Consejo Superior de Investigaciones Científicas, Isaac Newton 8, PTM Tres Cantos, 28760 Madrid, Spain
luisja@imm.cnm.csic.es

Abstract: This study investigates the dispersion relation of two dimensional photonic crystals conformed in a hybrid triangular-graphite configuration. This lattice includes, as limiting cases, two major well-known structures, the triangular and the graphite lattices. The analysis has been carried out by using preconditioned block-iterative algorithms for computing eigenstates of Maxwell's equations for periodic dielectric systems, using a plane-wave basis. We present the evolution of the so-called gap maps as a function of the radii of the structures. We conclude that a number of gaps exist for both TM and TE polarizations. We also predict the appearance of sizeable complete band gaps for structures the can be achieved using present fabrication capabilities.

OCIS codes: (260.2110) Electromagnetic theory, (220.4830) Optical systems design, (350.3950) Micro-optics

References and Links

1. E. Yablonovitch, "Inhibited spontaneous emission in solid-state physics and electronics," Phys. Rev. Lett. **58**, 2059-2062 (1987).
2. S. John, "Strong localization of photons in certain disordered dielectric superlattices," Phys. Rev. Lett. **58**, 2486-2489 (1987).
3. S.Y. Lin *et al*. "A three dimensional photonic crystal operating at infrared wavelenghts", Nature **394**, 251 (1998); A. Blanco, *et al.* "Large-scale synthesis of a silicon photonic crystal with a complete three-dimensional bandgap near 1.5 micrometres", Nature **405**, 437 (2000); Y. Vlasov, *et al*., "On-chip natural assembly of silicon photonic band gap crystals", **414,** 289 (2001).
4. R. D. Meade, K. L. Brommer, A. M. Rappe, and Joannopoulos, "Existence of a photonic band gap in two dimensions," Appl. Phys. Lett. **61**, 495-497 (1992).
5. D. Cassagne, C. Jouanin, and D. Bertho, "Photonic band gaps in a two-dimensional graphite structure," Phys. Rev. B **52**, R2217-R2220 (1995).
6. D. Cassagne, C. Jouanin, and D. Bertho, "Hexagonal photonic-band-gap structures," Phys. Rev. B **53**, 7134-7142 (1995).
7. R. Padjen, J. M. Gérad, and J. Y. Marzin, "Analysis of the filling pattern dependence of the photonic bandgap for two-dimensionl systems," J. Mod. Opt. **41**, 295-310 (1994).
8. S. G. Johnson and J. D. Joannopoulos, "Block-iterative frequency-domain methods for Maxwell's equations in planewave basis," Opt. Express **8**, no. 3, 173-190 (2001), http://www.opticsexpress.org/abstract.cfm?URI=OPEN-8-3-173.
9. S. G. Johnson and J. D. Joannopoulos, The MIT Photonic-Bands Package home page http://ab-initio.mit.edu/mpb/ .

1. Introduction

Since the pioneering works of Yablonovitch [1] and John [2] that proposed that certain periodic dielectric structures present a complete photonic band gap, these structures, nowadays known as photonic crystals, have generated considerable attention. For their possibilities in practical applications, three-dimensional photonic crystals exhibiting at least a complete band gap within the range of telecommunication frequencies have been intensely looked for [3]. However, light-based technological applications have their roots in planar technology, which requires a full knowledge of the band gap location in two dimensional

#5250 - $15.00 US Received 8 September 2004; revised 4 November 2004; accepted 4 November 2004

structures (considered infinitely long in the third dimension). Paradoxically, the theoretical study of such structures requires less effort than that of their three-dimensional counterparts. This is due to the fact that for two-dimensional structures, the wave propagation can be studied separately for two different polarizations, thus the original vector problem is split in two scalar problems. These polarizations are known as *transversal magnetic* (TM) if the electric field is perpendicular to the plane defining the structure and as *transversal electric* (TE) if this is the magnetic field. Several structures have been found to present gaps for one of these polarizations and some even for both of them simultaneously. A triangular lattice of air cylinders embedded in a dielectric material presents a large band gap for TE polarized waves and a complete one for large radius air cylinders [4]. The graphite structure, also for air cylinders, presents important gaps for the mode TM [5,6]. It has been proven that any deviation of the cylinders from a circular symmetry produces a reduction of the size of the gaps [7]. Both structures belong to the same Bravais lattice and show good properties for a different electromagnetic mode. Our aim is to take advantage of those properties by combining these two structures. For this purpose, we have constructed a hybrid triangular-graphite lattice by placing the air cylinder of the triangular lattice in the center of each honeycomb of the graphite structure (see Fig. 1). We have studied the gap positions obtained varying the values of the radii of the cylinders forming the triangular and graphite structures independently. We have considered the two possible situations: (i) the cylinders are made of air embedded in a dielectric matrix and (ii) the dielectric cylinders in air. Our simulations show the existence of an important number of gaps for both modes, as well as several complete gaps. Some of the complete gaps are found within the fabrication tolerance.

2. Structure description and simulations

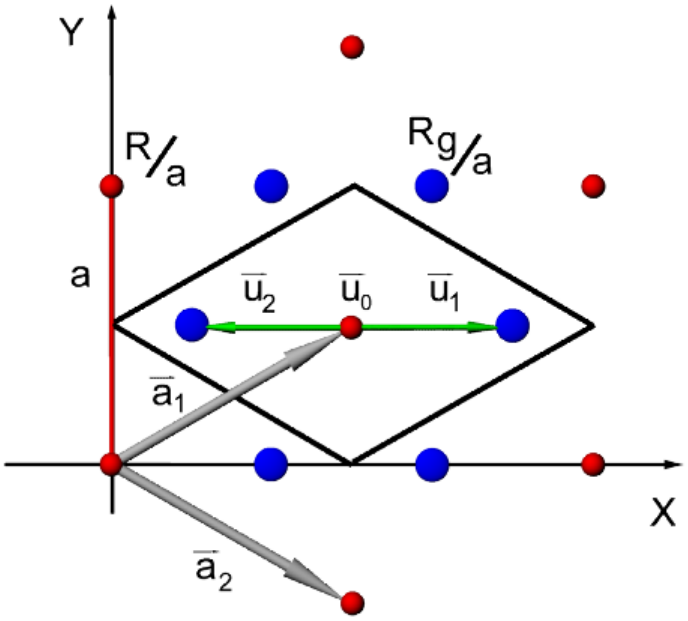

Fig. 1. Structure of the hybrid lattice under consideration. Small dots are at the position of the triangular lattice and have radii *R/a*, whereas big dots are located at the positions of a graphite structure and have radii *Rg/a*. The lattice parameter is *a* and the vectors defining the primitive cell are $\mathbf{a}_1$ and $\mathbf{a}_2$. The unit cell is delimited by the thick lines and contains three elements in its interior. These elements are located at $\mathbf{u}_0=\mathbf{0}$, $\mathbf{u}_1=(\mathbf{a}_1+\mathbf{a}_2)/3$ and $\mathbf{u}_0=-(\mathbf{a}_1+\mathbf{a}_2)/3$ with respect to the center of the unit cell.

The 2D periodic structure used throughout this work is depicted in Fig. 1. Let *R/a* be the radius of the cylinders of the triangular sub-lattice and *Rg/a* the radius of the cylinders of the

#5250 - $15.00 US Received 8 September 2004; revised 4 November 2004; accepted 4 November 2004

graphite sub-lattice, being *a* the lattice parameter. The hybrid triangular-graphite lattice is generated by means of triangular Bravais lattice with primitive vectors $\mathbf{a_1} = a\left(\sqrt{3}/2, 1/2\right)$ and $\mathbf{a_2} = a\left(\sqrt{3}/2, -1/2\right)$ and three cylinders by unit cell at positions (with respect to the center of the cell): $\mathbf{u_0} = \mathbf{0}$, $\mathbf{u_1} = \frac{(\mathbf{a_1} + \mathbf{a_2})}{3}$ and $\mathbf{u_2} = -\frac{(\mathbf{a_1} + \mathbf{a_2})}{3}$. The radius of the cylinder placed in $\mathbf{u_0}$ is *R/a* (its replication alone would give rise to the triangular lattice) and the radius of the cylinders placed in $\mathbf{u_1}$ and $\mathbf{u_2}$ is *Rg/a* (whose replication alone would give rise to a graphite type lattice). The distance between the center of nearest-neighbor cylinders is $a/\sqrt{3}$ and the conditions of non-overlapping cylinders are: $R/a \le 0.5$, $Rg/a \le 1/2\sqrt{3}$, and $R/a + Rg/a \le 1/\sqrt{3}$. When R/a is equal to *Rg/a* the hybrid triangular-graphite lattice becomes a triangular lattice with lattice parameter $a/\sqrt{3}$. Also, when *Rg/a* is equal to zero the standard triangular lattice is obtained, and when *R/a* is equal to zero we recover the usual graphite lattice. The variation of the values of *R/a* and *Rg/a* leads to different configurations for the hybrid triangular-graphite lattice.

The primitive vectors of the reciprocal lattice for the hybrid structure are $\mathbf{b_1} = 2\pi/a\left(\frac{1}{\sqrt{3}}, 1\right)$ and $\mathbf{b_2} = 2\pi/a\left(\frac{1}{\sqrt{3}}, -1\right)$, that gives to a hexagonal first Brillouin zone with the same symmetry points as the triangular or graphite lattice.

The hybrid structure that we want to discuss is completely described by giving the value of the radii *Rg/a* and *R/a*, and the dielectric constant ε. For ε we have chosen the value ε=10.24 since it is close to that of many semiconductors presenting interesting properties in the infrared domain.

In order to obtain the dispersion relations we have used a plane-wave expansion method consisting of the fully vectorial solution of Maxwell's equations with periodic boundary conditions computed by preconditioned conjugate-gradient minimization of the block Rayleigh quotient [8,9].

3. Photonic band gaps

In this section we will address the dispersion relations that form the structure described above. We are mainly interested in the band gap formation as a function of *R/a* and *Rg/a*. An example of dispersion relation for the hybrid structure is presented in Fig. 2 (*R/a=0.1* and *Rg/a=0.24* with ε=10.24). We can see that there are several partial gaps (i.e. those that open only for one polarization). For this particular choice of the parameters there is an especially wide band gap for TE modes opening at $\omega a/2\pi c \approx 0.45$ and also a complete band-gap at $\omega a/2\pi c \approx 0.82$.

In order to analyze the formation of the band-gaps for different values of the radii *R* and *Rg* we have calculated the evolution of the so-called gap-maps. The gap-maps show the position of the band-gap as a function of the radius of the structure. In our case we have two relevant radii, therefore we have performed two kind of evolutions. First, we have calculated the gap-maps for a fixed value of *R/a* (when *R/a*=0 the gap-map corresponds to that of the graphite structure) and then varied the value of *R/a*. We will refer to those as *graphite-gap-maps* (GGM). Second, we have done the same but inverting the order, performing then the *triangular-gap-maps* (TGM).

#5250 - $15.00 US Received 8 September 2004; revised 4 November 2004; accepted 4 November 2004

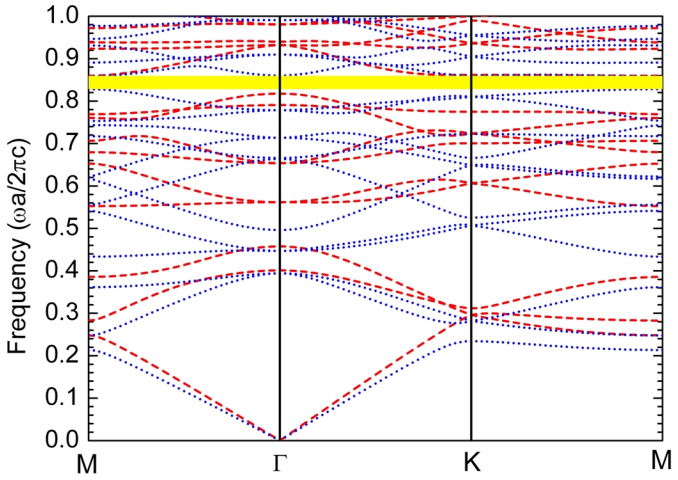

Fig. 2. Photonic band structure for TE (red long-dashed lines) and TM (blue dashed lines) polarization of the hybrid triangular-graphite structure of air holes in a dielectric matrix of index ε=10.24 for radius of the holes *R/a=0.1* and *Rg/a=0.24*. A complete band-gap is observed for a normalized frequency around 0.84 (shadowed area).

3.1 Hybrid triangular-graphite lattice of circular holes in a dielectric background

We have fixed a set of nineteen values between zero and 0.5 for *Rg/a* and we have varied *R/a* in the same range (evolution of the GGMs as a function of *R/a*), as it is shown in the animated plots of Fig. 3. In this way, starting from the graphite structure (*R/a=0*, see first frame in the left hand side of Fig. 3) we can follow the evolution of the gaps as the triangular sublattice grows in the structure. From the starting point there are two main TM (always in blue) gaps corresponding to the graphite lattice (the bare GGM). As *R/a* increases the range of extension of these two TM gaps decreases. At the same time a TE (always in red) gap opens in the radius range of non-overlapping cylinders ($x<R/a<y$) of the graphite sublattice. Both TM gaps disappear for *R/a*=0.25 and *R/a*=0.3 respectively, whereas the TE gap evolves in a complementary way. Eventually it mixes with other TM gaps producing several TEM gaps (for both TE and TM modes, in yellow in the plots) at normalized frequencies ranging between 0.7 and 0.9. The maximum size for this TE gap is for $Rg/a \approx R/a \approx 0.25$, which is the case of a triangular lattice with a reduced lattice parameter. From this point the size of the TE gap decreases, and for $R/a \approx 0.4$ it disappears completely, leaving a new TM gap. It is also interesting to observe the formation of a wide TE gap at low energies (0.2 to 0.5 of normalized frequencies) beginning in *R/a*=0.2 and reaching its maximum size at $R/a \approx 0.45$.

The widest TM gap appears for large values of *R/a* (*R/a*>0.375) and for values of *Rg/a* that produce overlapping between adjacent cylinders. The origin lies on the fact that for this range of values our structure is essentially a graphite lattice of dielectric rods in air of noncircular section (a six-point-star-like cross-section, but very close to circular). It is actually the graphite structure of circular dielectric rods for low volume fraction the one that presents TM mode gaps [5-6].

There are several values of *R/a* for which complete TEM gaps appear covering a significant range of normalized frequencies: from 0.8 to 1 for *R/a*=0.1, from 0.6 to 0.8 in the middle of the evolution (close to the reduced-lattice-parameter-triangular lattice case) and 0.4 to 0.55 at the end of the calculation, where a lattice formed by columns is achieved.

For *R/a*=0.1 a significant complete gap appears for high frequency. Inside this area, for *Rg/a*=0.24 the value of the complete gap is centered near $\omega a/2\pi c=0.84$ with a 3.6% of relative width (see Fig. 2). This configuration presents lattice dimensions within the fabrication

#5250 - $15.00 US Received 8 September 2004; revised 4 November 2004; accepted 4 November 2004

tolerances. For example, if we want a photonic gap centered at 1.5μm we have to set a=1.246μm, R=126nm and Rg=303nm. For those values the separation between the border area of nearest-neighbor cylinders is 123 nm, which is sufficiently thick to be fabricated using standard technologies for dry etching.

We have performed the same analysis but considering the TGMs as a function of the radius of the graphite sublattice (Right hand side of Fig. 3). For Rg/a = 0 the structure corresponds to the bare TGM and from there the gaps change as the graphite sublattice grows in the structure.

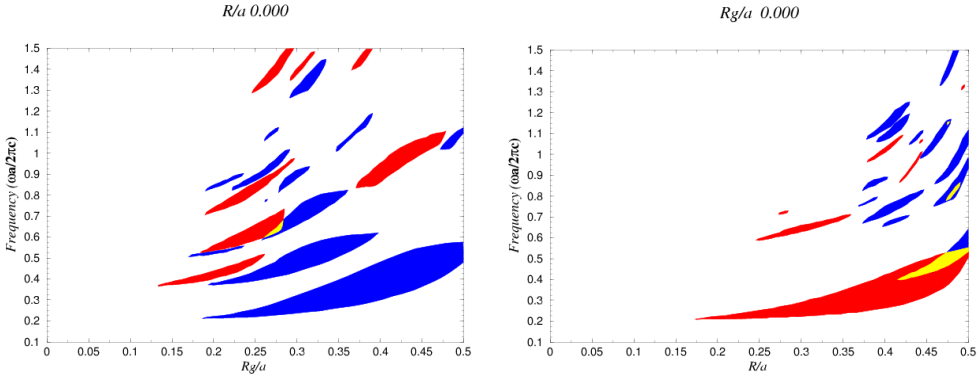

Fig. 3. Photonic band maps for the TE (red) polarization and TM (blue) polarization of a hybrid triangular-graphite structure of air cavities in a dielectric matrix of index ε=10.24. Left (275Kb animation): Graphite-lattice maps, varying the radius of the cylinders of the triangular lattice. Right (238Kb animation): Triangular lattice maps as the radius of the cylinders of the graphite sublattice grows.

The initial TGM presents the well known TE and TM gaps which overlap for a significant fraction near the *close-packed* condition. As Rg grows, the number and size of new gaps for the TM mode appear at different frequencies, reaching values of $\omega a/2\pi c$ as low as 0.2.

It is remarkable that a second TE gap, which is not present in the case of the bare TGM, appears in the hybrid lattice when Rg/a=0.075 for $\omega a/2\pi c$ around 0.45. The size of this gap grows as Rg/a increases, covering a range of normalized frequencies from $\sim 0.45<\omega a/2\pi c<0.8$. At the same time the TE gap corresponding to the bare triangular lattice vanishes. When $Rg/a\approx 0.25$, this gap reaches its maximum size for a value of $R/a\approx 0.25$. Again, this is the case of the reduced-lattice-parameter triangular lattice. This gap is also responsible of the formation of two important complete TEM gaps for values of Rg/a between 0.25 and 0.275. For values of $Rg/a>0.275$, the holes of the graphite lattice begin to overlap. As mentioned above, it is now when the TM gaps become "dominant" since the structure is essentially made of dielectric rods in air.

3.2 Hybrid triangular-graphite lattice of rods in air

Figure 4 shows the change of the band gaps of the hybrid lattice for the case of rods in air. We have fixed again nineteen values within the same range as in Section 3.1 to obtain the evolution of the gaps. In the left hand side of Fig. 4, we see the evolution of the GGMs. As it can be expected, most of the gaps correspond to the TM type, but there is an important number of TE gaps exhibiting a considerable size. These TE gaps contribute to produce several complete TEM gaps for relatively high energies ($\omega a/2\pi c\approx 1$) when the R/a grows.

#5250 - $15.00 US Received 8 September 2004; revised 4 November 2004; accepted 4 November 2004

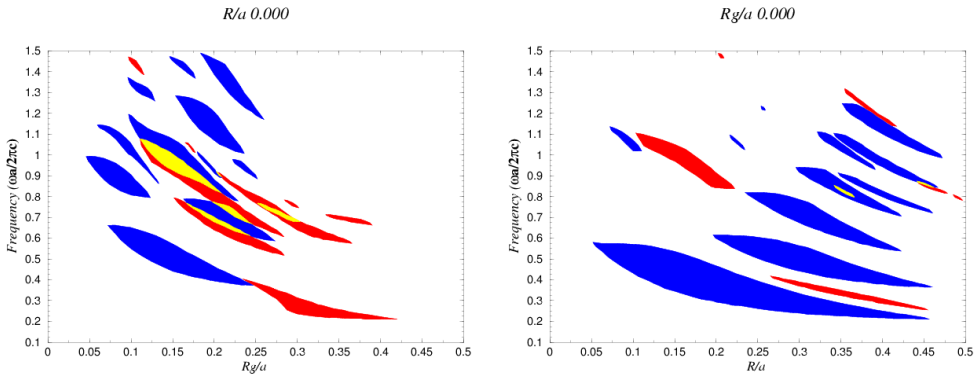

Fig. 4. Photonic band maps for the TE (red) polarization and TM (blue) polarization of a hybrid triangular-graphite structure of dielectric rods in air. Left (245Kb animation): GGMs, varying the radius of the cylinders of the triangular lattice. Right (228Kb animation): TGMs as the radius of the cylinders of the graphite sublattice increases.

The right hand side of Fig. 4 contains the evolution of the hybrid lattice when the rods corresponding to the graphite lattice change their radius (0<Rg<0.5). Since the starting point is the bare TGM we observe the large of TM gaps characteristic of this structure, along with some TE gaps. The evolution shows that the size of the TM gaps is noticeable, with such a number and distribution that almost all the space in the plot corresponds to areas inside a gap, reaching a maximum for Rg between 0.15 and 0.20. In this case the appearance of complete TEM gaps as Rg grows appear in a more clear way. It is worth noticing that their number and extension is especially relevant for Rg between 0.050 to 0.250. The TEM gaps appear also at high energies, which can be interesting from a technological point of view because the lattice parameter gets larger. Despite the problem of the confinement in the third dimension existing in actual devices, this lattice displays characteristics that makes it a very interesting structure for the realization of practical devices.

4. Summary

We have investigated the photonic bandgaps associated to a hybrid two-dimensional triangular-graphite lattice in which the radii of the two lattices have been varied. A wide range of TE , TM and complete TEM gaps with significant sizes have been found for different normalized frequencies and for different values of the radii, within reasonable fabrication tolerances. The new geometries found may allow the fabrication of structures with extended photonic properties.

Acknowledgments

We want to thank Dr. C. López from the ICMM-CSIC for computation time. A. García-Martín and P.A. Postigo would like to thank the support of a “Ramón y Cajal” contract from the Spanish Ministry of Science and Technology. We want also to thank research projects CAM 07N/0059/02, CICYT TIC2002-04096-C03-03 and DPI2001-0024-C03-01 for providing a fellowship for L.J. Martínez.